European Review for Medical and Pharmacological Sciences 2019; 23: 9625-9632

Effects of ranolazine on cardiac function in rats with heart failure

G.-T. WANG[1,2], H. LI[2], Z.-Q. YU[2], X.-N. HE[3]

[1]Daqing Campus of Harbin Medical University, Daqing, China
[2]Department of Cardiology, the Fourth Hospital of Daqing City, Daqing, China
[3]Emergency Citical Care Center, Beijing AnZhen Hospital, Capital Medical University, Beijing, China

Abstract. – OBJECTIVE: To investigate the effects of ranolazine on the cardiac function and myocardial apoptosis in rats with heart failure and its possible mechanisms.

MATERIALS AND METHODS: Thirty Wistar rats were randomly divided into sham operation (negative control; NC), chronic heart failure (CHF), and ranolazine groups. Suprarenal abdominal aortic coarctation was used to induce CHF in rats. Five weeks later, rats in the ranolazine group received ranolazine (50 mg/kg) daily, whereas those in the CHF group received normal saline. After 4 weeks, changes in hemodynamic parameters, cardiac structure and pathology, myocardial apoptosis, and protein expression were assessed.

RESULTS: The left ventricular end-diastolic pressure (LVEDP) significantly increased in the CHF group; whereas the maximal rate of left ventricular pressure rise and fall (±dp/dtmax) decreased, compared to those in the NC group. Ranolazine significantly reduced LVEDP and increased ±dp/dtmax (p<0.01), compared to those in the CHF group. Severe impairment of cardiomyocytes was observed in the CHF group with evident inflammation; however, ranolazine reversed these deficits. Rats in the CHF group exhibited an increase in TUNEL-positive cells, which was inhibited by ranolazine, where the apoptotic index significantly decreased in ranolazine-treated rats (p<0.01). Also, ranolazine downregulated caspase-9 expression and upregulated pAKT and Bcl-2 expression in rat cardiomyocytes. Moreover, ranolazine significantly inhibited myocardial apoptosis and caspase-9 expression, promoted AKT phosphorylation, and upregulated pAKT and Bcl-2 expression *in vitro*, compared to those in the control group (p<0.001). LY294002 inhibited ranolazine-induced suppression of myocardial apoptosis (p<0.001).

CONCLUSIONS: Ranolazine improved cardiac function and inhibited myocardial apoptosis in rats with CHF, which could be attributed to the regulation of AKT phosphorylation.

Key Words:
Ranolazine, Heart failure, Myocardial apoptosis, AKT, pAKT.

Introduction

Heart failure is a cardiovascular syndrome caused by cardiac systolic or diastolic dysfunction. In end-stage heart disease, heart failure often manifests as pulmonary congestion, venous stasis, and dyspnea[1,2]. Heart failure seriously affects the normal cardiopulmonary function and is closely related to myocardial ischemia and apoptosis[3]. Clinically, angiotensin-converting enzyme inhibitors (ACEI), angiotensin receptor blockers (ARB), beta-blockers, and mineralocorticoid receptor antagonists are used to assist cardiac resynchronization therapy[4,5]. Among these, drugs, such as ivabradine, ranolazine, and cardiac myosin agonists, have been commonly used in clinical practice. Ranolazine, an anti-ischemic piperazine derivative, selectively inhibits the late Na^+ current in cardiomyocytes[6,7]. Recently, ranolazine has been shown to play an important role in improving myocardial diastolic function and treating diastolic heart failure; however, the underlying mechanisms of action are still unclear. In this study, we aimed to investigate the effects of ranolazine on cardiac function and myocardial apoptosis in rats with heart failure and elucidate its potential mechanisms of action.

Materials and Methods

Materials

Thirty specific-pathogen-free (SPF) male Wistar rats (6-8 weeks old, weighing 180 ± 20 g) were purchased from Experimental Animal Center of the Academy of Military Medical Sciences (Beijing, China). They were kept in cages at an SPF laboratory animal center. The experimental procedures were conducted in accordance with the regulations of the Animal Welfare Act and were approved by The Fourth Hospital of Daqing

Corresponding Author: Xiaonan He, Ph.D; e-mail: iceboy8899@163.com

City Ethics Committee. The following reagents were used: ranolazine hydrochloride (Sigma-Aldrich, St. Louis, MO, USA), adjusted to a final concentration of 50 mg/mL before use; sodium pentobarbital (Sigma-Aldrich, St. Louis, MO, USA); terminal deoxynucleotidyl transferase-mediated dUTP-biotin nick end labeling (TUNEL) kit (Promega, Madison, WI, USA); proteinase K (Shanghai Yisheng, Shanghai, China); radioimmunoprecipitation assay (RIPA) lysate and bicinchoninic acid (BCA) protein assay kits (Beyotime, Shanghai, China); goat anti-rabbit IgG, anti-glyceraldehyde 3-phosphate dehydrogenase (GAPDH), anti-AKT, anti-pAKT, anti-caspase-9, and anti-Bcl-2 (Abcam, Cambridge, MA, USA); phosphate-buffered saline (PBS), trypsin, fetal bovine serum, and Dulbecco's Modified Eagle's Medium (DMEM)-F12 medium (Gibco, Rockville, MD, USA); LY294002 (CST, Danvers, MA, USA); and enzyme-linked immunosorbent assay (ELISA)^{PLUS} kit (Roche, Basel, Switzerland).

Establishment of the Animal Model

After one-week acclimatization, rats were randomly divided into sham operation, chronic heart failure (CHF) model, and ranolazine groups (10 rats/group). The sham operation, CHF, and ranolazine groups were used as negative control (NC), positive control, and experimental groups, respectively. Three groups of rats were used to establish a heart failure model using the suprarenal abdominal aortic coarctation procedure, as previously described[8]. Rats in the three groups were anesthetized with an intraperitoneal injection of 3% (mass fraction) sodium pentobarbital at a ratio of 0.15 mL/100 g and fixed in the supine position. Hair removal and disinfection were carried out before making an incision along the abdominal midline. The abdominal wall was cut open layer by layer, and the abdominal aorta was isolated and partially ligated to reduce its diameter by approximately 50%. The patency of the aorta was confirmed before a layered closure of the abdominal wall was performed. In the sham operation group, the abdominal aorta was isolated but not ligated. Penicillin (200,000 U) was intraperitoneally administered daily for 3 consecutive days after the operation.

Criteria for Successful Modeling and Dosing Regimen

During routine feeding, the food intake, body weight changes, and routine activity of the rats in the three groups were recorded. After five weeks, rats with CHF developed loss of appetite, depression, slow weight gain or even weight loss, and hair loss. The model of left ventricular chronic pressure overload was considered successful if the left ventricular end-diastolic pressure (LVEDP) reached 15 mmHg (1 mmHg = 0.133 kPa). After successful model establishment, CHF rats were divided into the CHF or ranolazine experimental groups. Rats in the experimental group were administered 50 mg/kg ranolazine daily for 4 weeks, whereas those in the sham operation and CHF groups were administered the same amount of normal saline. At the end of the experiment, the rats were sacrificed. For each rat, a tissue block of the left ventricular anterior wall (1 mm × 1 mm × 1 mm) was sampled, fixed in 5% paraformaldehyde, and stored at room temperature until their use. Additionally, heart tissue (100 mg) was stored in liquid nitrogen until use.

Isolation, Culture, and Grouping of Myocardial Cells From Rats With Heart Failure

After successful modeling, heart tissues (0.5 cm × 0.5 cm × 0.5 cm) were harvested from each rat in the CHF group, and the myocardial cells were isolated with trypsin[9]. The isolated cells were purified by differential adherence and chemical inhibition with bromodeoxyuridine (BrdU)[10]. The cells were routinely cultured in DMEM-F12 complete medium containing 20% fetal bovine serum at 37°C using a 5% CO_2 incubator. When the cell density reached approximately 85%, the cells were subcultured and divided into three groups: the control (Ctr), ranolazine-treated (Ran), and ranolazine plus LY294002, a specific inhibitor of the PI3K/AKT pathway, (Ran+LY294002) groups. Cells in the Ctr group were not treated, whereas cells in the Ran group were treated with 100 μM ranolazine, and cells in the Ran+LY294002 group were treated with 50 μM LY294002 after treatment with 100 μM ranolazine. Cells were then collected for subsequent experiments.

Hemodynamic Measurements of Changes in Cardiac Function

Body weight of rats in each group was measured 4 weeks after drug administration, and rats were then anesthetized with an intraperitoneal injection of 3% (mass fraction) sodium pentobarbital at a ratio of 0.15 mL/100 g, and fixed in the supine position. The left ventricle was retrogradely intubated through the right com-

mon carotid artery and connected to the pressure transducer. Hemodynamic signals were recorded using a multimedia biosignal acquisition system to determine LVEDP and the maximal rate of left ventricular pressure rise and fall ($\pm dp/dt_{max}$) values. LVEDP reflects the preload of ventricular contraction. The lower the LVEDP value, the better the myocardial diastolic function. $+dp/dt_{max}$ reflects the myocardial contractile function. The greater the $+dp/dt_{max}$ value, the better the myocardial contractile function. Similarly, the $-dp/dt_{max}$ reflects the myocardial diastolic function. A larger value indicates better myocardial diastolic function.

Histopathological Examination of Heart Tissues by HE Staining

After fixation for 6-8 h, the tissue blocks of the left ventricular anterior wall were embedded in paraffin and sectioned (5-μm slices) along the coronal plane. Histopathological changes in the hearts of rats in each group were observed by hematoxylin and eosin (HE) staining (Boster, Wuhan, China).

Determination of Myocardial Apoptotic Index by TUNEL Assay

The sections were deparaffinized, fully hydrated using gradient alcohol flooding, incubated with proteinase K at room temperature for 20 min, and washed with PBS for 3 times (5 min each). The TUNEL reagent was then added for 1 h 37°C. Diaminodiphenyl (DAB) was used for 10 min for color development. The sections were rinsed with PBS until they became colorless to avoid non-specific color development, dried, and mounted in neutral balsam. Under a high-power microscope (400×), 5 fields/section were randomly selected and counted. The nuclei of positive cells were stained brown. The total cell count and positive cell count (mean value of 5 selected fields) for each section were recorded, and the apoptotic index (AI) was calculated. AI = (positive cell count / total cell count) × 100%.

Determination of Protein Expression in Heart Tissues by Western Blot Analysis

RIPA lysate containing 1 mM phenylmethylsulfonyl fluoride (PMSF) was added to approximately 50 mg of frozen heart tissue. Then, they were homogenized at 4°C and incubated on ice for 20 min. The homogenate was centrifuged at 12,000 rpm at 4°C for 15 min, and the supernatant was collected. After quantification using the BCA protein assay kit, 100 mg of protein was mixed with 5× Sodium Dodecyl Sulfate (SDS) loading buffer at a 4:1 ratio, and the proteins were denatured in a boiling water bath for 5-10 min. Proteins were subjected to 10% SDS-polyacrylamide gel electrophoresis (PAGE), transferred to a polyvinylidene difluoride (PVDF) membrane (Millipore, Billerica, MA, USA), incubated with antibodies, and transferred to a gel imager for detection of the target protein bands.

Determination of Apoptosis by ELISA^{PLUS} Kit

After treatment, cells from each group were collected, mixed with 200 L of cell lysate for 30 min at room temperature. The mixture was centrifuged at 2000 rpm for 10 min, and 20 μL of the supernatant was added to the ELISA plate wells with 6 repetitions for each group. In addition, 20 μL of histone-DNA complex was added to an additional well as a positive control. Determination of apoptosis was carried out using the ELISA^{PLUS} kit, according to the manufacturer's protocol. The absorbance of each well at 405 and 490 nm was measured by dual-wavelength colorimetry. The content of histone-DNA fragments was expressed as the mean value of absorbance (OD value).

Statistical Analysis

All data were statistically analyzed using the Statistical Product and Service Solutions (SPSS) 19.0 software (IBM, Armonk, NY, USA). Data were expressed as the means ± standard deviations. The *t*-test was used for pairwise comparisons, and one-way analysis of variance (ANOVA) was used for multiple-group comparisons, followed by Post-Hoc Test (Least Significant Difference). $p<0.05$ was considered statistically significant.

Results

Changes in Hemodynamic Parameters Among Groups

LVEDP significantly increased in rats of the CHF and ranolazine groups, whereas $\pm dp/dt_{max}$ significantly decreased ($p<0.01$), compared to those in the sham operation group (NC). After 4-week ranolazine administration, LVEDP significantly decreased in rats of the ranolazine group, whereas $\pm dp/dt_{max}$ significantly increased ($p<0.01$), compared to those in the CHF group (Table I).

Pathological Changes in The Heart Tissues of Rats Examined by HE Staining

HE-stained heart tissues were examined using high-power (400×) light microscopy. As shown in Figure 1, the myocardial cells of rats in the NC group were arranged tightly and regularly with normal morphology, clear tissue structures, and no infiltration of inflammatory cells. However, the heart tissues of rats in the CHF group developed severe lesions. Figure 1B shows that the myocardial cells were hypertrophied and disordered with unclear structures and partial infiltration of inflammatory cells. The pathological changes observed in rats of the ranolazine group were significantly less severe, compared to those in the CHF group; however, myocardial edema, adhesion, and unclear structures were still observed. No tissue inflammation was detected.

Changes in AI Among Groups

Using TUNEL staining, apoptotic cell nuclei were stained brown. As shown in Figure 2, apoptotic cells were rare in rats of the NC group. Myocardial cells were arranged tightly and regularly, and the nuclei were evenly dispersed. There were more apoptotic nuclei in the CHF and ranolazine groups than those in the NC group. As shown in Table II, the AI values of the CHF and ranolazine groups were significantly higher than that of the NC group ($p<0.01$). Also, rats in the ranolazine group showed less intense nuclear staining and a significant decrease in the number of myocardial apoptotic cells (AI), compared to those in the CHF group ($p<0.01$).

Changes in Myocardial Protein Expression Among Groups

Western blot analysis was used to determine the expression levels of AKT, pAKT, caspase-9, and Bcl-2 in the myocardial tissues of rats in all groups. As shown in Figure 3, there was no significant difference in the expression level of AKT among groups. The expression levels of pAKT and Bcl-2 were the highest in the ranolazine group, and there was a significant difference in pAKT and Bcl-2 expression between the ranolazine and CHF group ($p<0.001$). The expression levels of caspase-9 in both the CHF and ranolazine groups increased, compared to that in the NC group. However, caspase-9 expression was significantly lower in myocardial tissues of rats from the ranolazine group than that in the CHF group ($p<0.001$).

Table I. Comparison of hemodynamic parameters of three groups of rats ($\bar{x}\pm s$).

Group	Cases	LVEDP (mmHg)	+dp/dt$_{max}$ (mmHg/s)	-dp/dt$_{max}$ (mmHg/s)
NC	10	4.97 ± 0.83	6031.50 ± 214.09	4830.51 ± 177.05
CHF	10	18.07 ± 2.11*	4270.19 ± 183.80*	2649.02 ± 118.60*
Ranolazine	10	12.42 ± 1.75$^{*\#}$	4966.57 ± 149.73$^{*\#}$	3433.56 ± 159.54$^{*\#}$

Note: $^{*}p< 0.01$ compared with the NC group; $^{\#}p<0.01$ compared with the CHF model group. LVEDP: left ventricular end-diastolic pressure; +dp/dt$_{max}$: the maximal rate of left ventricular pressure rise; -dp/dt$_{max}$: the maximal rate of left ventricular pressure decline; 1 mmHg = 0.133 kPa

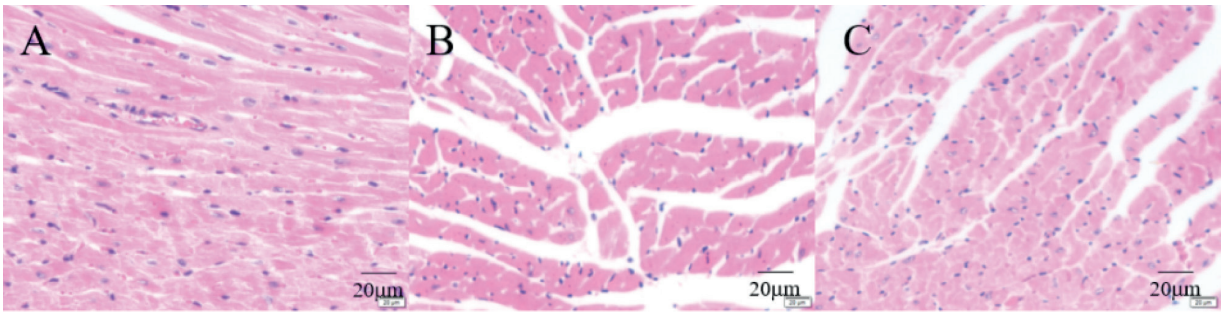

Figure 1. Pathological changes in myocardial cells of rats from all groups, examined by HE staining using light microscopy (400×). **A,** NC group; **B,** CHF model group; **C,** ranolazine group.

Table II. Myocardial apoptosis index of three groups of rats.

Group	Cases	AI (%)
NC	10	3.01 ± 0.86
CHF	10	56.31 ± 3.22*
Ranolazine	10	17.95 ± 1.70*#

Note: *p<0.01 compared with the NC group; #p<0.01 compared with the CHF model group.

Determination of Myocardial Apoptosis In Vitro by ELISAPLUS

As shown in Figure 4, the number of myocardial apoptotic cells was the highest in the Ctr group. Ranolazine significantly decreased myocardial apoptosis, compared to that in the Ctr group (p<0.001). Concurrent administration of LY294002 significantly increased the number of apoptotic cells, compared to that in the Ran group (p<0.001). There was no significant difference between the Ran+LY294002 and Ctr groups (p>0.05).

Changes in Myocardial Protein Expression Among Groups In Vitro

As shown in Figure 5, treatment with ranolazine or LY294002 *in vitro* did not affect AKT expression in myocardial cells (p>0.05). However, treatment with ranolazine significantly increased the expression levels of pAKT and Bcl-2, whereas concurrent treatment with LY294002 significantly inhibited the expression of pAKT and Bcl-2, compared to those of the Ran group (p<0.001). Moreover, ranolazine inhibited the expression of caspase-9 in myocardial cells, whereas concurrent treatment with LY294002 significantly increased the expression of caspase-9, compared to that in the Ran group (p<0.001).

Discussion

CHF is one of the most common critical illnesses in clinical practice with a complicated pathogenesis. Most patients with CHF have a history of heart diseases, including coronary heart disease, hypertension, and myocarditis[11,12]. Recently, there is increasing belief that CHF is associated with ventricular remodeling, the neuroendocrine system, and various humoral factors[13,14]. Current clinical therapies include diuretics, nitrates, and cardiac stimulants according to the different causes of CHF[3]. Specifically, ventricular remodeling is directly affected by ventricular myocardial apoptosis[15]. Abnormal apoptosis of myocardial cells can result from the abnormal activation of the inherent cellular death program by certain stimulating factors in the myocardial cells. Myocardial cells of patients with heart failure undergo remodeling of their energy metabolism with blocked cellular metabolism. The accumulation of colony-stimulating factors promotes myocardial apoptosis, eventually leading to ventricular remodeling. Therefore, inhibition of the expression of apoptosis-stimulating factors and reduction of myocardial apoptosis may be a potential mechanism for the treatment of CHF.

In this study, ranolazine was administered to rats with heart failure, and the cardiac function, hemodynamics, myocardial AI, and expression levels of apoptosis-related proteins were assessed to investigate the possible application of ranolazine in the treatment of heart failure. Moreover, the mechanism underlying the antiapoptotic effects of ranolazine was further verified by *in vitro* culture of impaired myocardial cells with ranolazine and LY294002. Results showed that the LVEDP value of the CHF group was 18.07 ± 2.11 mmHg, indicating that CHF rat model was successfully established. Ranolazine could significantly improve the cardiac function of rats and increase the $\pm dp/dt_{max}$ value, compared to those of the CHF group (Table I). HE staining showed that treatment with ranolazine could ameliorate the pathological changes in the myocardial tissue (Figure 1). Determination of myocardial AI by TUNEL staining showed that the number of TUNEL-positive cells in the ranolazine group was significantly reduced, and AI was significantly lowered (Figure 2, Table II). Western blot analysis showed that ranolazine promoted AKT phosphorylation and increased the expression of the anti-apoptotic factor, Bcl-2; however, it did not affect AKT expression. The expression level of caspase-9 in the myocardial tissues of rats in the ranolazine group significantly decreased, compared to that in the CHF group (p<0.001). Isolated myocardial cells from CHF rats were cultured *in vitro* and treated with ranolazine or ranolazine+LY294002. As shown in Figures 5, ranolazine inhibited myocardial apoptosis, promoted the expression of pAKT and Bcl-2, and inhibited the expression of caspase-9 *in vitro*. LY294002 blocked ranolazine-induced inhibition of apoptosis. The number of apoptotic cells was significantly higher in the ranolazine+LY294002 group than that in the Ran group, and there was

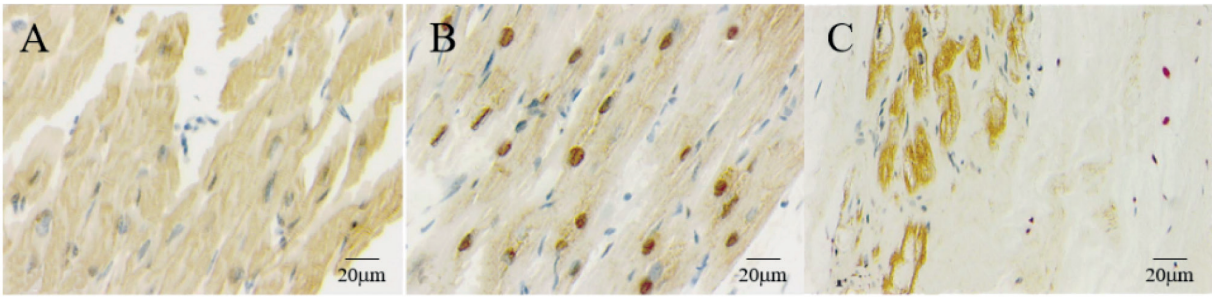

Figure 2. Myocardial apoptosis in rats of all groups, visualized by TUNEL staining (400×). **A,** NC group; **B,** CHF model group; **C,** ranolazine group.

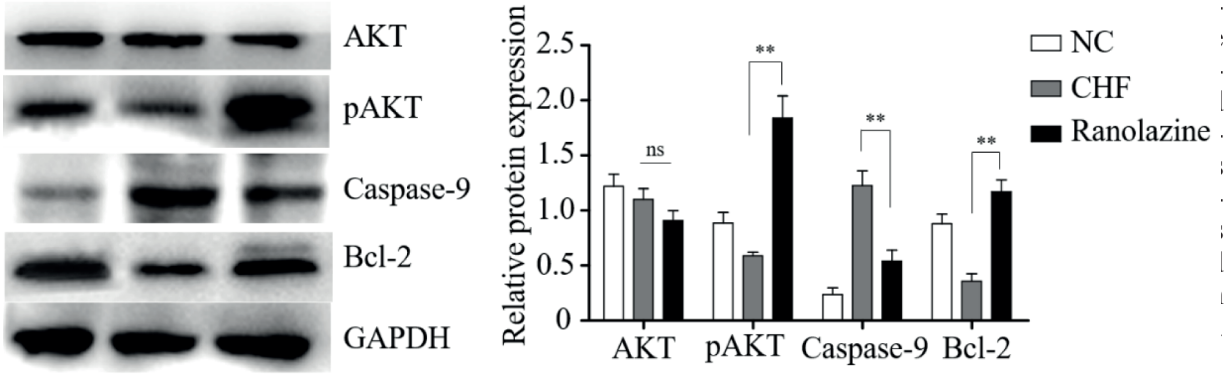

Figure 3. Determination of expression levels of myocardial proteins in rats of all groups by Western blot analysis. $^{ns}p>0.05$, compared to the CHF model group; $^{**}p<0.001$, compared to the CHF model group.

no significant difference in the number of apoptotic cells between the ranolazine+LY294002 and Ctr groups. Moreover, LY294002 inhibited AKT phosphorylation, compared to that in the Ran group ($p<0.001$). Also, LY294002 inhibited the expression of Bcl-2 and promoted the expression of caspase-9. Neither ranolazine nor LY294002 had any effect on AKT expression.

According to previous studies[16,17], the PI3K/AKT signaling pathway is closely related to heart failure. Activation of PI3K promotes phosphorylation of AKT and activates downstream signaling. It plays an important role in the cardiovascular system, myocardial apoptosis, and metabolism. In this work, we showed that administration of ranolazine promoted AKT phosphorylation, as evidenced by the significant increase in pAKT expression. AKT is an important downstream kinase regulated by PI3K, and an increase in pAKT/AKT ratio suggests that the PI3K-AKT pathway is activated, possibly promoting the recruitment of myocardial protective factors. In addition, we showed that ranolazine could inhibit the expression of the proapoptotic factor, caspase-9 and promote that of the antiapoptotic protein, Bcl-2 owing to inhibition of the mitochondrial apoptotic pathway, eventually inhibiting myocardial apoptosis. Referring to the previous literature[18,19], we speculated that ranolazine might inhibit the activation of the proapoptotic molecule, Bcl-2/Bcl-XL-associated death promoter (BAD) by promoting AKT phosphorylation, which result-

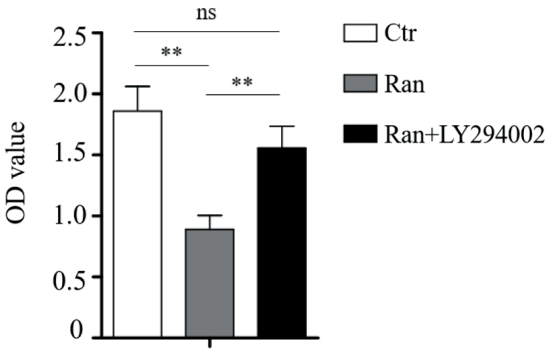

Figure 4. Determination of the effects of ranolazine/LY294002 on myocardial apoptosis *in vitro* by ELISA^{PLUS}. Pairwise comparison, $^{ns}p>0.05$, $^{**}p<0.001$.

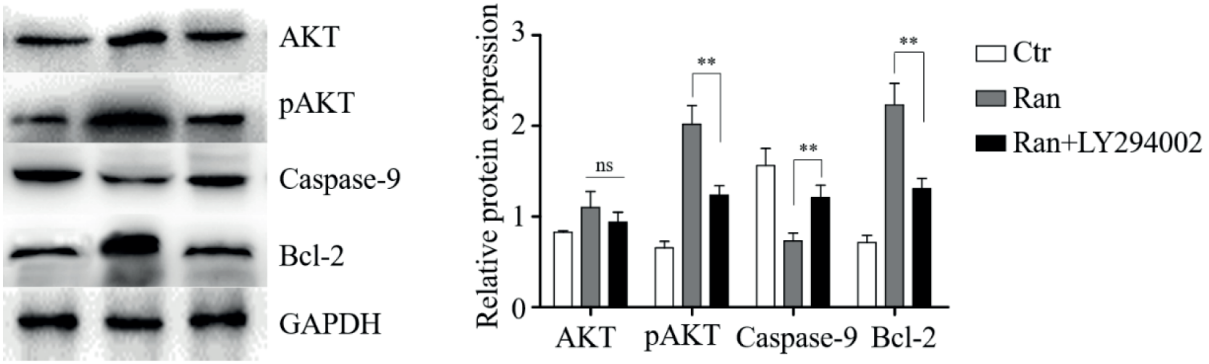

Figure 5. Determination of the effects of ranolazine/LY294002 on the expression of related myocardial proteins by Western blot analysis. $^{ns}p>0.05$, compared to the CHF model group; $^{**}p<0.001$, compared to the CHF model group.

LY294002 is a specific inhibitor of the PI3K/AKT pathway[20]. LY294002 prevents the activation of AKT and downstream signaling pathways by inhibiting AKT phosphorylation, which reduces cell viability and promotes myocardial apoptosis. The results of this investigation showed that LY294002 could significantly block the antiapoptotic effects of ranolazine, mainly by inhibiting AKT phosphorylation and regulating the expression of related proteins, such as caspase-9 and Bcl-2.

Conclusions

We showed that ranolazine could improve the cardiac function, reverse myocardial pathological changes, slow ventricular remodeling, and inhibit myocardial apoptosis in rats with heart failure. The underlying mechanism might be closely related to the regulation of AKT phosphorylation, affecting the activation of the PI3K/AKT signaling pathway.

Conflict of Interests

The Authors declare that they have no conflict of interests.

References

1) Gedela M, Khan M, Jonsson O. Heart failure. S D Med 2015; 68: 403-405, 407-409.
2) Zhou SL, Zhang J, Song TT, Li X, Wang HX. Diagnostic accuracy of natriuretic peptides for acute heart failure: a review. Eur Rev Med Pharmacol Sci 2018; 22: 2415-2420.
3) Testa G, Cacciatore F, Bianco A, Della-Morte D, Mazzella F, Galizia G, Gargiulo G, Curcio F, Liguori I, Sabusco A, Rengo F, Bonaduce D, Abete P. Chronic obstructive pulmonary disease and long-term mortality in elderly subjects with chronic heart failure. Aging Clin Exp Res 2017; 29: 1157-1164.
4) Rinkuniene D, Krivickiene A, Laukaitiene J, Jurkevicius R. Pharmacological treatment changes of chronic heart failure during cardiac resynchronization therapy: A 1-year follow-up study. Int J Cardiol 2017; 238: 92-96.
5) Witt CT, Kronborg MB, Nohr EA, Mortensen PT, Gerdes C, Nielsen JC. Optimization of heart failure medication after cardiac resynchronization therapy and the impact on long-term survival. Eur Heart J Cardiovasc Pharmacother 2015; 1: 182-188.
6) De Angelis A, Cappetta D, Piegari E, Rinaldi B, Ciuffreda LP, Esposito G, Ferraiolo FA, Rivellino A, Russo R, Donniacuo M, Rossi F, Urbanek K, Berrino L. Long-term administration of ranolazine attenuates diastolic dysfunction and adverse myocardial remodeling in a model of heart failure with preserved ejection fraction. Int J Cardiol 2016; 217: 69-79.
7) Rosano G, Vitale C, Volterrani M. Pharmacological management of chronic stable angina: focus on ranolazine. Cardiovasc Drugs Ther 2016; 30: 393-398.
8) Cappetta D, Esposito G, Coppini R, Piegari E, Russo R, Ciuffreda LP, Rivellino A, Santini L, Rafaniello C, Scavone C, Rossi F, Berrino L, Urbanek K, De Angelis A. Effects of ranolazine in a model of doxorubicin-induced left ventricle diastolic dysfunction. Br J Pharmacol 2017; 174: 3696-3712.
9) Hayama K, Maruyama N, Abe S. Cell preparation method with trypsin digestion for counting of colony forming units in Candida albicans-infected mucosal tissues. Med Mycol 2012; 50: 858-862.
10) Yan N, He Y, Wen H, Lai F, Yin D, Cui H. A Suzuki-Miyaura method for labelling proliferating cells containing incorporated BrdU. Analyst 2018; 143: 1224-1233.

11) Saitoh M, Dos SM, Emami A, Ishida J, Ebner N, Valentova M, Bekfani T, Sandek A, Lainscak M, Doehner W, Anker SD, von Haehling S. Anorexia, functional capacity, and clinical outcome in patients with chronic heart failure: results from the Studies Investigating Co-morbidities Aggravating Heart Failure (SICA-HF). ESC Heart Fail 2017; 4: 448-457.
12) Allida SM, Inglis SC, Davidson PM, Lal S, Hayward CS, Newton PJ. Thirst in chronic heart failure: a review. J Clin Nurs 2015; 24: 916-926.
13) Swedberg K. Importance of neuroendocrine activation in chronic heart failure. Impact on treatment strategies. Eur J Heart Fail 2000; 2: 229-233.
14) Peng Y, Ou BQ, Li HH, Zhou Z, Mo JL, Huang J, Liang FL. Synergistic effect of atorvastatin and folic acid on cardiac function and ventricular remodeling in chronic heart failure patients with hyperhomocysteinemia. Med Sci Monit 2018; 24: 3744-3751.
15) Liang T, Zhang Y, Yin S, Gan T, An T, Zhang R, Wang Y, Huang Y, Zhou Q, Zhang J. Cardio-protecteffect of qiliqiangxin capsule on left ventricular remodeling, dysfunction and apoptosis in heart failure rats after chronic myocardial infarction. Am J Transl Res 2016; 8: 2047-2058.
16) Siman FD, Silveira EA, Fernandes AA, Stefanon I, Vassallo DV, Padilha AS. Ouabain induces nitric oxide release by a PI3K/Akt-dependent pathway in isolated aortic rings from rats with heart failure. J Cardiovasc Pharmacol 2015; 65: 28-38.
17) Cantoni S, Cavallini C, Bianchi F, Bonavita F, Vaccari V, Olivi E, Frascari I, Tassinari R, Valente S, Lionetti V, Ventura C. Rosuvastatin elicits KDR-dependent vasculogenic response of human placental stem cells through PI3K/AKT pathway. Pharmacol Res 2012; 65: 275-284.
18) Verrier RL, Kumar K, Nieminen T, Belardinelli L. Mechanisms of ranolazine's dual protection against atrial and ventricular fibrillation. Europace 2013; 15: 317-324.
19) Li J, Wu H, Xue G, Wang P, Hou Y. 17beta-oestradiol protects primary-cultured rat cortical neurons from ketamine-induced apoptosis by activating PI3K/Akt/Bcl-2 signalling. Basic Clin Pharmacol Toxicol 2013; 113: 411-418.
20) Sun H, Xu B, Sheveleva E, Chen QM. LY294002 inhibits glucocorticoid-induced COX-2 gene expression in cardiomyocytes through a phosphatidylinositol 3 kinase-independent mechanism. Toxicol Appl Pharmacol 2008; 232: 25-32.